Novel E-O Modulation and Applications
THz Technology
BSPA Competition
RoF Systems
Optical Laser andTransmitter
MWP Applications
Novel High Speed Components
MWP Signal Processing
UWB System and Applications
Functional Devices
Relative Applications

APMP 2009

Technical Program

Asia-Pacific Microwave Photonics Conference

April 22-24, 2009
Beijing International Conventional Center
Beijing, China

Friday, 24 April, 2009

Conference Hall No. 303

14:20-14:35

L03- ***Ring defect photonic crystal vertical cavity surface emitting laser***

Anjin Liu, Hongwei Qu, Wei Chen, Mingxin Xing, Wenjun Zhou, and Wanhua Zheng
Nano-optoelectronics Lab, Institute of Semiconductors, CAS, Beijing, China

Abstract: Selectively oxidized ring defect photonic crystal vertical cavity surface emitting laser (RD-PCVCSEL) is demonstrated. The device achieves coherent coupling over the entire continuous-wave current range.

14:35-14:50

L04- ***CMOS Integrated Optical Receivers for Radio-over-Fiber Transmission of IEEE 802.11g WLAN Signals***

Jin-Sung Yoon, Hyo-Soon Kang, Myung-Jae Lee, Kang-Yeob Park, and Woo-Young Choi
Department of Electrical and Electronic Engineering, Yonsei University, 134 Shinchon-dong, Seodaemoon-gu, Seoul 120-749, Korea

Abstract: This paper presents an integrated optical receiver fabricated with 0.13-¦Ìm standard complementary metal-oxidesemiconductor (CMOS) technology for cost-effective radio-overfiber (RoF) systems. The CMOS integrated optical receiver is composed of a CMOS-compatible avalanche photodetector (CMOS-APD) and a transimpedance amplifier (TIA) circuits. Using a negative capacitance cell, gain and bandwidth of the CMOS integrated optical receiver are enhanced. The power dissipation (excluding output buffer) and the core size of the fabricated receiver are about 18 mW at 1.2 V supply voltage and 0.38 x 0.38 mm2, respectively. With this integrated optical receiver, radio-over-fiber transmission of IEEE 802.11g 54-Mb/s WLAN signals at 2.4 GHz is achieved with 3.89 % error vector magnitude.

14:50-15:05

L05- ***RF Distortion Effects on a Fiber Ring Based Optical Frequeny Comb Generator***

P. Shen, N. J. Gomes and P. A. Davies
Department of Electronics, University of Kent, Canterbury, Kent, CT2 7NT, UK

Abstract: This paper discusses the effect of distortion in the RF reference signal used to drive an Optical Frequency Comb Generator. It is demonstrated that the optical comb spectral profile can be significantly altered by the amplitude and phase of the RF harmonics of the drive signal.

15:05-15:25 **Coffee Break**

15:25-17:00 **Session M: Relative Applications**

Session Co-chairs:
Prof. Kun Qiu, (University of Electronic Science and Technology of China, China)
Dr. Li Xia (Nanyang Technological University, Singapore)

15:25-15:50

M01- ***Semiconductor Optical Amplifier-Enabled Intensity Modulation of Adaptively Modulated Optical OFDM signals for Passive Optical Networks (Invited)***

J.M.Tang
School of Electronic Engineering, Bangor University, UK

Abstract: The feasibility of using Semiconductor Optical Amplifiers (SOAs) to achieve intensity modulation of adaptively modulated optical orthogonal frequency division multiplexed (AMOOFDM) signals will be presented for practical applications in WDM PONs. It will be shown that the optimized SOA-based intensity modulators can offer colorless operation and support a 30Gb/s AMOOFDM signal transmission over a 80km SMF, which doubles the transmission performance offered by directly modulated DFB lasers. The aforementioned performance enhancement is mainly due to a considerable reduction in the frequency chirp effect, resulting from the strong SOA gain saturation-induced bandwidth broadening. Relatively low extinction ratio and clipping of the SOA modulated signals are identified to be the key factors limiting the maximum achievable AMOOFDM transmission performance.

CMOS Integrated Optical Receivers for Radio-over-Fiber Transmission of IEEE 802.11g WLAN Signals

Jin-Sung Yoon, Hyo-Soon Kang, Myung-Jae Lee, Kang-Yeob Park, and Woo-Young Choi
Department of Electrical and Electronic Engineering
Yonsei University
134 Shinchon-dong, Seodaemoon-gu, Seoul 120-749, Korea
wchoi@yonsei.ac.kr

***Abstract*—This paper presents an integrated optical receiver fabricated with 0.13-μm standard complementary metal-oxide-semiconductor (CMOS) technology for cost-effective radio-over-fiber (RoF) systems. The CMOS integrated optical receiver is composed of a CMOS-compatible avalanche photodetector (CMOS-APD) and a transimpedance amplifier (TIA) circuits. Using a negative capacitance cell, gain and bandwidth of the CMOS integrated optical receiver are enhanced. The power dissipation (excluding output buffer) and the core size of the fabricated receiver are about 18 mW at 1.2 V supply voltage and 0.38 × 0.38 mm^2, respectively. With this integrated optical receiver, radio-over-fiber transmission of IEEE 802.11g 54-Mb/s WLAN signals at 2.4 GHz is achieved with 3.89 % error vector magnitude.**

I. INTRODUCTION

Complementary metal-oxide-semiconductor (CMOS) technology has been used for all the electronic applications including analog, digital, and radio frequency integrated circuits due to its advantages of high integration level, high performance, and low fabrication cost. In addition, with silicon photodetectors operating at 850-nm, CMOS-based optoelectronics have been regarded as a promising solution for short-distance optical access networks, optical interconnects, and radio-over-fiber (RoF) systems [1-4]. By using CMOS technology, a fully integrated optical receiver having a photodetector as well as necessary electronic circuits can be implemented in a cost effective manner.

Previously, CMOS-compatible avalanche photodetectors (CMOS-APDs) were utilized for remote antenna units in RoF systems [5]. With a readily available AlGaAs/GaAs vertical-cavity surface-emitting laser (VCSEL) and multimode fiber (MMF) as an optical transmitter and a transmission medium, respectively, low-cost RoF downlinks for cellular and/or wireless local area network (WLAN) services were successfully demonstrated. However, as of yet, single chip integration of the entire optical receivers for remote antenna units is still challenging owing to the bandwidth limitation of CMOS-compatible photodetectors (CMOS-PDs).

In this work, we present a CMOS integrated optical receiver having a CMOS-APD and a transimpedance amplifier (TIA) circuit for RoF transmission of 2.4-GHz IEEE 802.11g WLAN data signals. To overcome the limited bandwidth of the CMOS-APD, the gain-bandwidth enhancement technique using a negative capacitance is adopted for the TIA circuit. The integrated optical receiver is fabricated with 0.13-μm standard CMOS technology. For feasibility demonstration of RoF systems using the CMOS integrated optical receiver, downlink data transmission of 54-Mb/s 64 quadrature amplitude modulation (QAM) orthogonal frequency-division multiplexing (OFDM) WLAN data signals at 2.4 GHz is performed with a VCSEL, MMF, and 1-m long wireless link. Furthermore, performance evaluation for the CMOS integrated optical receiver is carried out with error vector magnitude (EVM) measurements with varying the CMOS-APD bias voltage and optical modulation index.

II. CMOS INTEGRATED OPTICAL RECEIVER

A. CMOS-Compatible Avalanche Photodetector

The CMOS-APD is implemented by a p-n junction between p+ source/drain and n-well regions. The details of the device structure can be found in [6]. In order to block slow diffusion currents generated in p-substrate regions, photocurrents are collected by p+ regions. Multi-finger electrodes with 0.5-μm spacing are employed on the active area for the exclusion of the lateral diffusion path. The active area of the CMOS-APD is about 30 × 30 μm^2 and the optical window is formed by blocking the salicide process during the fabrication.

For the characterization of the CMOS-APD, output currents are measured at the p+ contact with the applying bias voltage to the n-well contact. All the experiments for the

This research was supported by Ministry of Knowledge Economy under the IC Design Education Center (IDEC) Support Program (MPW, CAD) and Dongbu HiTek Semiconductor.

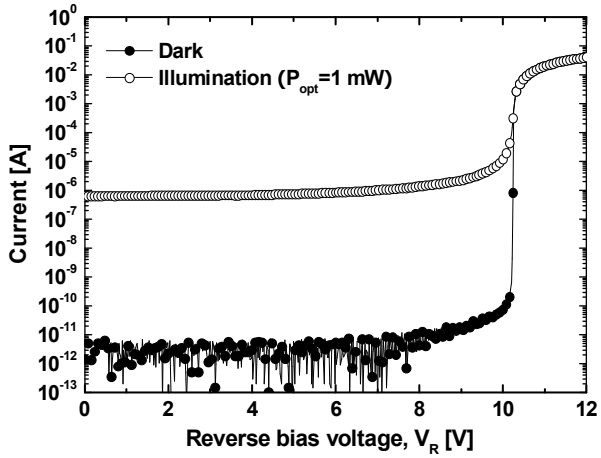

Figure 1. Current-voltage characteristics of the CMOS-APD as a function of the reverse bias voltage (V_R) under dark and illumination conditions. Incident optical power (P_{opt}) is 0 dBm.

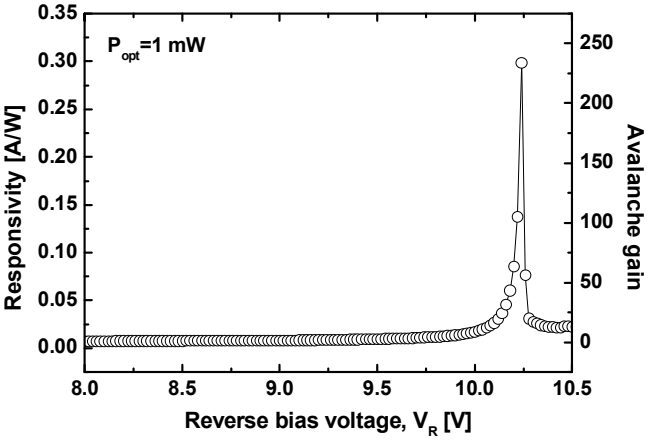

Figure 2. Responsivity and avalanche gain of the CMOS-APD as a function of the reverse bias voltage (V_R). Incident optical power (P_{opt}) is 0 dBm.

CMOS-APD are done on-wafer. Current-voltage (I-V) characteristics of the CMOS-APD as a function of the reverse bias voltage (V_R) under dark and illumination conditions are shown Fig. 1. In the device, it is observed that avalanche breakdown starts to occur at the bias voltage of about 10.1 V under dark condition. Fig. 2 shows responsivity and avalanche gain of the CMOS-APD. With the maximum avalanche gain of about 234, the CMOS-APD provides high responsivity of 0.324 A/W at the reverse bias voltage of 10.24 V.

B. Transimpedance Amplifier

In the CMOS integrated optical receiver, output photocurrents of the CMOS-APD are converted to voltage signals with amplification by transimpedance gain. Fig. 3 shows the simplified structure of the CMOS integrated optical receiver and core schematic of the feedback amplifier. In the feedback amplifier, high feedback resistance (R_F) is required to reduce input-referred noises, which, however, can limit the bandwidth. In order to simultaneously achieve high sensitivity and large bandwidth of optical receivers, high feedback

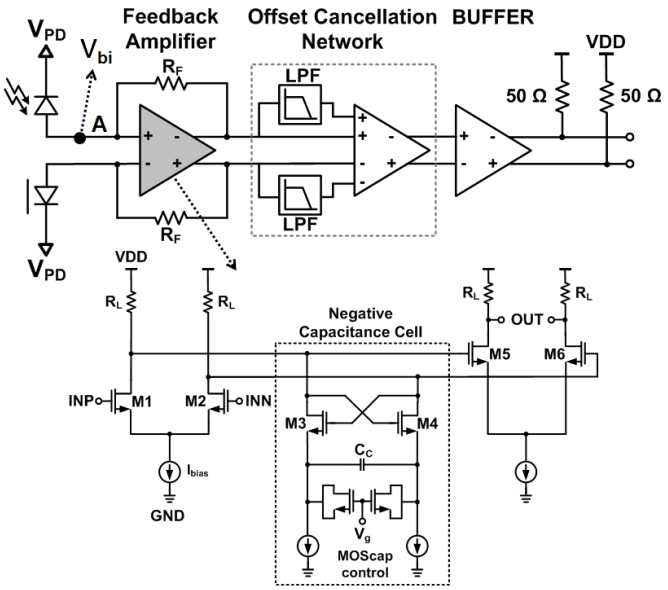

Figure 3. Configuration of CMOS integrated optical receiver and core schematic of feedback amplifier with negative capacitance cell.

resistance of 2 kΩ and a negative capacitance cell are adopted as shown in Fig. 3. In the feedback amplifier, the negative capacitance is controlled by the gate voltage of the metal-oxide-semiconductor (MOS) capacitor. As the gate voltage increases from 0.6 to 1.2 V, capacitance of the MOS capacitor increases to enhance the bandwidth of optical receiver. The input of the TIA (point A in Fig. 3) is biased at the built-in voltage (V_{bi}) of about 1 V. Because differential TIA input is connected to a single-ended photodiode input, the output of the TIA generates pseudo-differential signals. To convert this pseudo-differential output into fully-differential signals, an offset cancellation network having two low-pass filters (LPFs) and f_T-doubler is designed. Operating under 1.2 V supply voltage, the power dissipation of the integrated optical receiver is 18 mW excluding the output buffer and the CMOS-APD. The core size of the fabricated optical receiver is 0.38 × 0.38 mm^2. The chip is glued on a test circuit board and their terminals bond wired to PCB signal lines.

Photodetection frequency responses of the integrated optical receiver are measured using a vector network analyzer (50Ω reference). Fig. 4 shows the result at the photodetector bias voltage of 10.1 V. Despite the limited bandwidth of 1.85 GHz in the CMOS-APD, the integrated optical receiver provides 3-dB bandwidth of 2.01 GHz with the help of the negative capacitance at the minimum gate bias voltage of the MOS capacitor (V_g) of 0.6 V. By increasing V_g, thus increasing capacitance, 3-dB bandwidth of the optical receiver is extended up to 2.51 GHz and photodetected signal power at 2.4 GHz is increased about 6 dB at maximum V_g of 1.2 V. From the photodetection frequency responses, transimpedance gain of TIA circuits is measured as shown in Fig. 4. The difference of responses between CMOS-APD and optical receiver indicates transimpedance of about 500 Ω. Compared with feedback resistance of TIA circuits, R_F= 2 kΩ, the measured transimpedance from frequency responses is

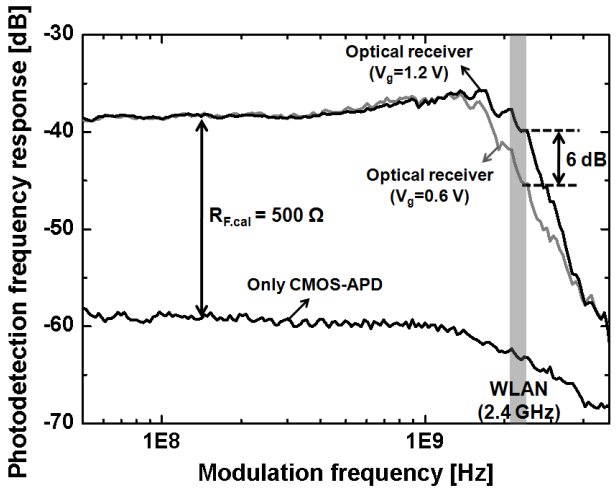

Figure 4. Photodetection frequency responses of the CMOS integrated optical receiver and CMOS-APD. Incident optical power (P_{opt}) is 0 dBm.

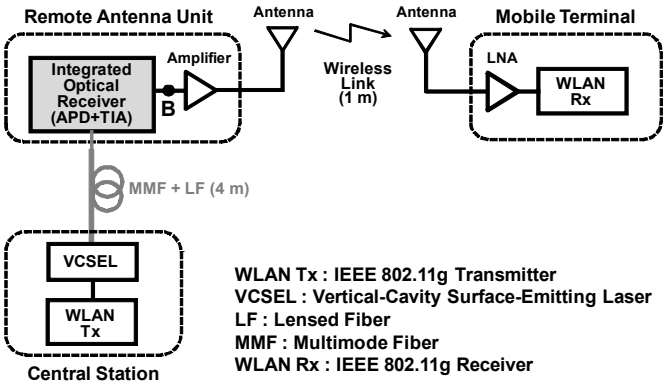

Figure 5. Experimental setup for RoF data transmission.

reduced by the factor of four due to the output buffer and single-ended output connection for the measurement.

III. RoF Transmission of 2.4-GHz IEEE 802.11g WLAN Signal Using the CMOS Integrated Optical Receiver

Using the integrated CMOS optical receiver, IEEE 802.11g 54-Mb/s WLAN data transmission at 2.4 GHz is performed. Fig. 5 shows the experimental configuration for RoF downlink data transmission for IEEE 802.11g WLAN data signals. At the central station, WLAN data signals are generated from Anritsu MG3700A vector signal generator. 54-Mb/s 802.11g uses OFDM of 52 sub-carriers, each of which is modulated with 64 QAM. These signals are directly modulated using a VCSEL and transmitted through 4-m long multimode fiber and lensed fiber. At the remote antenna unit, output signals of the integrated optical receiver are amplified by a 24-dB gain broadband amplifier to compensate wireless link loss. The wireless link consists of two 4-dBi gain omnidirectional antennas and about 1-m free space. At the mobile terminal, received signals are amplified with a 24-dB

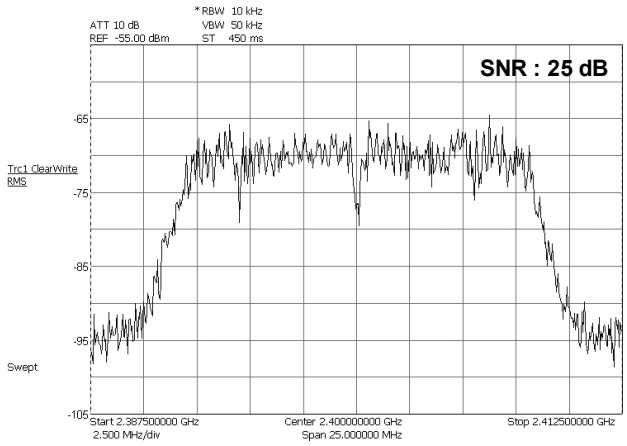

Figure 6. Output spectrum of the integrated optical receiver at B in Fig. 5.

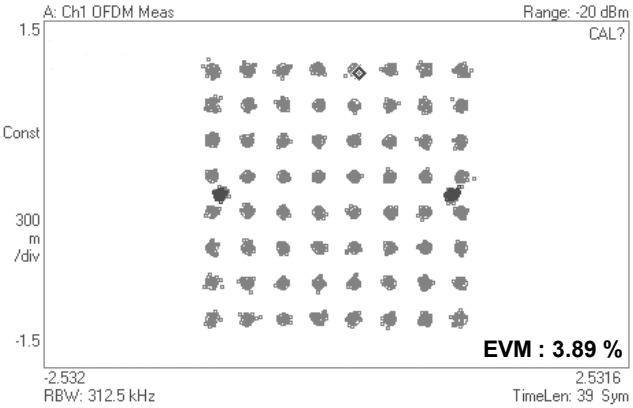

Figure 7. Constellation of demodulated WLAN data signals.

gain low-noise amplifier (LNA). For signal demodulation, LNA output signals are applied to an Agilent 89600 vector signal analyzer (VSA).

IV. Experimental Results

Fig. 6 and Fig. 7 show the output spectrum of the optical receiver (point B in Fig. 5) and constellation of demodulated WLAN data signals at the mobile terminal, respectively. The measured EVM is 3.89 %, where input RF signal power of -2 dBm and optical power of 1 dBm. For the data rate of 54 Mb/s, the relative constellation RMS error is restricted to 5.6 % in IEEE 802.11g standard [7]. Measured EVM results are satisfied with IEEE 802.11g EVM specification.

For the optimization of the CMOS integrated optical receiver performance, dependence of EVM for demodulated data and optical receiver output power for 2.4-GHz continuous-wave (CW) signal on bias voltage (V_{PD}) is investigated and the results are shown in Fig. 8. The optimum bias voltage for minimum EVM is slightly different from maximum output power condition. Optical receiver output power for 2.4-GHz CW signal is maximized at V_{PD} = 11.3 V, whereas EVM for demodulated signal is minimized at V_{PD} = 11.1 V. This discrepancy is attributed to the increased noise

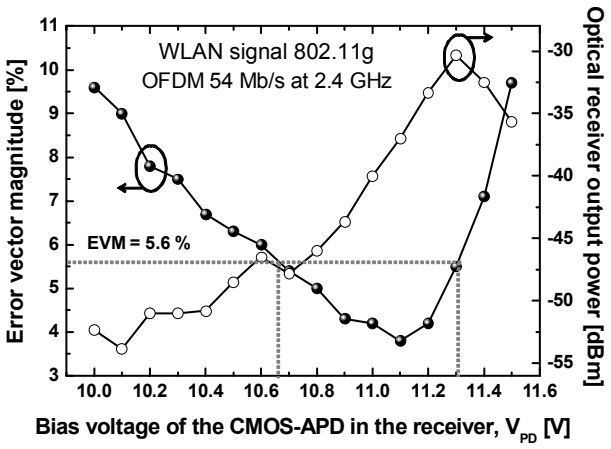

Figure 8. EVM of WLAN 802.11g demodulated data and optical receiver output power of 2.4 GHz continuous-wave (CW) signals as a function of bias voltage of the CMOS-APD in the optical receiver with -2 dBm of input RF signal power (P_{mod}).

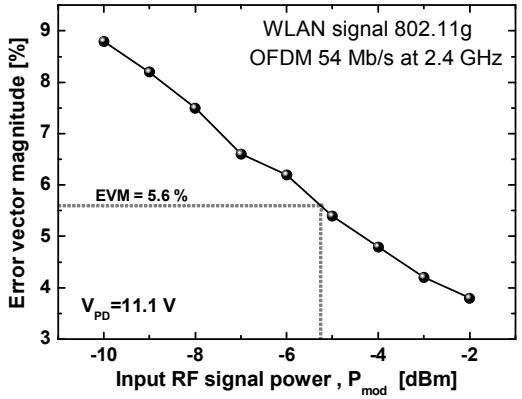

Figure 9. EVM as a function of input RF signal power at maximum SNR bias voltage of APD (V_{PD}=11.1 V).

power at 11.3V. With increasing bias voltage above 11.1 V, the receiver output power is increased due to enhanced avalanche gain. However, the noise also increases owing to multiplied dark currents. At V_{PD} below 10.7 V, measured EVM is also higher than specification because optical receiver output signal is too low to meet required SNR. From 10.7 V to 11.3 V, measured EVM satisfies the EVM specification of IEEE 802.11g (EVM < 5.6 %). Fig. 9 shows measured EVM as a function of input RF signal power into the VCSEL. For successful WLAN data signals transmission with fulfilling the EVM requirement, sufficient input RF power above -5 dBm is required to increase the optical modulation index.

In the experiment, the required input optical power into the integrated optical receiver is about 1 dBm. Because of this high output optical power requirement, RoF data transmission distance is limited. In order to transmit RoF data transmission with the low incident optical power, a higher sensitivity CMOS integrated optical receiver at the remote antenna unit is required. To increase sensitivity of the CMOS integrated optical receiver, high responsivity of the CMOS-APD and low input-referred noise of the TIA are important factors.

V. CONCLUSION

The CMOS integrated optical receiver is fabricated with 0.13-μm standard CMOS process. Bandwidth of the CMOS-APD is enhanced using negative capacitance in the TIA circuit. Using the integrated optical receiver, data transmission of IEEE 802.11g 54-Mb/s 64 QAM WLAN data signals at 2.4 GHz is successfully demonstrated for 1-m wireless link.

REFERENCES

[1] K. A. Persson, C. Carlsson, A. Alping, A. Haglund, J. S. Gustavsson, P. Modh, and A. Larsson, "WCDMA radio-over-fibre transmission experiment using singlemode VCSEL and multimode fibre," Electron Lett., vol. 42, pp. 372–374, March 2006.

[2] M. L. Yee, L. C. Ong, C. K. Sim, B. Luo, and A. Alphones, "Low-cost radio-over-fiber in-building distribution network for WLAN, UWB and digital TV broadcasting," in Proc. Asia-Pacific Microwave conference, pp. 95–98, December 2006.

[3] T. Niiho, M. Nakaso, K. Masuda, H. Sasai, K. Utsumi, and M. Fuse, "Multi-channel wireless LAN distributed antenna system based on radio-over-fiber techniques," The 17th annual meeting lasers and Electro-optics society., pp. 57–58, November 2004.

[4] M. Sauer and A. Kobyakov, "Low-cost radio-over-fiber links," The 20th annual meeting lasers and Electro-optics society., pp. 333–334, October 2007.

[5] H.-S. Kang, M.-J. Lee, and W.-Y. Choi, "Multi-standard radio-over-fiber systems using CMOS-compatible Si avalanche photodetectors," IEEE Topical Meeting on Microwave Photonics, pp. 302–305, September 2008.

[6] H.-S. Kang, M.-J. Lee, and W.-Y. Choi, "Si avalanche photodetectors fabricated in standard complementary metal-oxide-semiconductor process," Applied Physics Letters, vol. 90, pp. 151118-1–151118-3, April 2007.

[7] IEEE Std. 802.11g, "Further higher-speed physical layer extension in the 2.4 GHz band," 2003.